

***Final Draft***  
**of the original manuscript:**

Bellosta von Colbe, J.M.; Metz, O.; Lozano, G.A.; Pranzas, K.P.; Schmitz, H.W.; Beckmann, F.; Schreyer, A.; Klassen, T.; Dornheim, M.:

**Behavior of scaled-up sodium alanate hydrogen storage tanks during sorption**

In: International Journal of Hydrogen Energy (2011) Elsevier

DOI: [10.1016/j.ijhydene.2011.03.153](https://doi.org/10.1016/j.ijhydene.2011.03.153)

*Title:* Behaviour of scaled-up sodium alanate hydrogen storage tanks during sorption

*Authors:* Bellosta von Colbe, José M.<sup>\*a</sup>; Metz, Oliver<sup>a</sup>; Lozano, Gustavo A.<sup>a</sup>; Pranzas, P. Klaus<sup>a</sup>; Schmitz, Heinz W.<sup>a</sup>; Beckmann, Felix<sup>a</sup>; Schreyer, Andreas<sup>a</sup>; Klassen, Thomas<sup>a</sup>; Dornheim, Martin<sup>a</sup>

\* Corresponding author

<sup>a</sup>Helmholtz Zentrum Geesthacht, Centre for Materials and Coastal Research GmbH.  
Max Planck St. 1, 21502 Geesthacht, Germany

*E-mail:* [jose.bellostavoncolbe@hzg.de](mailto:jose.bellostavoncolbe@hzg.de), [oliver.metz@hzg.de](mailto:oliver.metz@hzg.de),  
[gustavo.lozano@hzg.de](mailto:gustavo.lozano@hzg.de), [klaus.pranzas@hzg.de](mailto:klaus.pranzas@hzg.de), [heinz.schmitz@hzg.de](mailto:heinz.schmitz@hzg.de),  
[felix.beckmann@hzg.de](mailto:felix.beckmann@hzg.de), [andreas.schreyer@hzg.de](mailto:andreas.schreyer@hzg.de), [thomas.klassen@hzg.de](mailto:thomas.klassen@hzg.de),  
[martin.dornheim@hzg.de](mailto:martin.dornheim@hzg.de).

### *Abstract*

Sodium alanate is being experimentally tested in scaled-up quantities. For this purpose, several tanks have been designed and constructed. The tank functionality during absorption and desorption of hydrogen was demonstrated in a scale of 8 kg of alanate, with a peak technical absorption time below 10 min. The absorption and desorption data show good reproducibility. Neutron radiography was used in another tank to show the powder's physical behaviour during sorption, showing conservation of the macroscopic structure during cycling.

*Keywords:* hydrogen storage, sodium alanate, tank, scale-up, in-situ neutron radiography.

### *Introduction*

Hydrogen as an energy vector has been discussed as the most promising alternative to fossil fuels, with a special emphasis on its storage [1, 2] for some time. Since no known storage method or material has been able to reach the targets set either in Europe or in the USA for light-duty vehicles [3, 4], this is still an important research field. However, the focus has shifted lately from basic investigation into materials to more applied systems [5]. In this frame, development and scale-up of known materials into practical tanks and systems starts to take precedence. In this work, the behaviour of two tanks, one with ~8 kg and the other with ~100 g sodium alanate is presented. The first one was designed and built in the frame of the EU STORHY

project and is being thoroughly tested within another EU project, NESSHY. The design, as well as simulation results regarding its sorption behaviour have been published elsewhere [6, 7]. The type of tank selected was a different one from similar efforts in the USA [8], since a tube-and-shell construction with the alanate in the tubes, although somewhat heavier, would lead to better heat transfer and avoidance of hot spots, with better kinetics as a result. Since demonstration of good kinetics was the main driver of the design at the time, the compromise reached between hydrogen sorption kinetics and tank weight was a good one. This has been vindicated by the hydrogen sorption results shown here, which represent the main novelty of the work.

### *Material and Methods*

The hydrogen storage material used in this work was sodium alanate doped with  $\text{TiCl}_3 \cdot \text{AlCl}_3$ , following the synthesis described elsewhere [9, 10]. A full description of the tank design, steel used, and other parameters, has already been published [6]. For the testing of the 8 kg alanate tank and subsequent designs, a new lab has been designed and built. In order to maximize safety, the testing chamber was equipped with explosion-safe devices, as well as a venting system for overpressure events. Fig. 1 shows the tank connected to the testing setup inside the explosion-resistant testing chamber.

### Fig. 1

The lab contains all measuring equipment (pressure gauges, mass flow controllers, thermocouples), as well as the electronics, valves, computer system and the auxiliary equipment. This consists of two subsystems: a hydrogen supply subsystem for pressures up to 130 bar using hydrogen of 99.999 % purity and a heat transfer system for operation temperatures up to 180 °C. The standard operation conditions are  $p_{\text{max}} = 100$  bar and  $T = 125$  °C for charging;  $p_{\text{min}} = 0.2 - 10$  bar and 160 - 175 °C for discharging the tank. In order to measure the hydrogen absorption curves shown below, the tank is brought to the operational temperature of 125 °C by means of heat transfer system using an oil flow of ~130 kg/min. Then, mass flow controllers let the selected flow of hydrogen pass into the tank, so that the pressure increases up to the desired level (100 bar). During the whole procedure, hydrogen flow, pressure and oil temperature are monitored and recorded at intervals of 0.5 sec. For the hydrogen

desorption, the procedure is similar, with the difference that the temperature is 160 °C and the hydrogen flow reverses its direction, coming out of the tank. When a pressure of 0.2 barg is reached and the flow of hydrogen negligible, the data acquisition is stopped.

### *Results and discussion*

The design of the 8 kg alanate tank was optimized regarding the minimization of hydrogen charging time [6]. The goal in this respect was a charging time of less than 10 minutes for 80 % of the capacity. Fig. 2 shows that this has been achieved in the 12<sup>th</sup> absorption. Cycles 1 to 10 were activation cycles and are therefore not considered here.

Fig. 2

In this figure, it can be seen that the charging process is divided into three regions: one from 0 to 0.5 wt %, where the charging speed is highest, one from 0.5 to 2.1 wt %, which shows a somewhat lower charging speed, and one from 2.1 to the final capacity of 3.7 wt %. The first region corresponds to an increase in pressure inside the tank vessel, without chemical reaction. The second region is due to the first step of the reaction leading to the formation of  $\text{Na}_3\text{AlH}_6$  (combined with a further increase in pressure), while the third region accounts for the second step of the reaction leading to the formation of  $\text{NaAlH}_4$  and the increase to the final pressure of 100 bar. Both capacity and speed of charging are in good agreement with previous data from lab-scale reactors [9, 11] and milligram scale samples measured in Sieverts' – type apparatus, showing that the scale-up of the system does not have adverse effects on its behaviour, and indicating that further scale-up is possible without degradation of storage properties.

At this point it is important to distinguish between material capacity and total capacity. The former gives the amount of hydrogen being stored in the hydride, bound as a chemical compound. The latter includes this plus the amount of hydrogen that remains in the gas phase inside the tank at the end of the loading procedure. As can be seen in Fig. 3, these amounts differ by some 0.6 wt % (around 13 % of the total capacity).

Fig. 3

Since the hydrogen in the gas phase will also be used in the application to which the tank is attached, it is reasonable to include it in the calculation of the available amount of hydrogen. Additionally, the system capacity is another metric of interest in this respect. It takes the amount of hydrogen available and divides it by the weight of the tank (hull plus metal hydride). The test tank used here was optimized for high rate of absorption only and not for light weight, thus it has a system capacity of some 0.8 wt %. In Fig. 3 it is also clearly visible that the material capacity curve has a change in slope at around 0.8 wt %. This corresponds to the change from the first to the second reaction step as previously mentioned. The change in slope is not evident in the total capacity curve because the lower hydrogen absorption into the material was compensated by a pressure increase.

Another important target in the evaluation of the tank is to ascertain that the results obtained during testing are reproducible. In order to do this, a series of absorption experiments was carried out under the same experimental conditions. These conditions were 125 °C, 2 to 100 bar of pressure, and the limitation to a maximum normal hydrogen flow rate of 240 L<sub>n</sub> min<sup>-1</sup> using a mass flow controller. The results of the three repetitions are shown in Fig. 4.

Fig. 4

Considering the slope of the curves, it becomes evident that the speed of the absorption reaction is nearly the same for the three charging processes, as is to be expected since it is limited by the hydrogen flow available from the mass flow controller.

On the other hand, the capacity increases with the cycle number. This is probably due to an activation process. It has been shown by Gross et al. [12] that, in some cases, up to 10 cycles are necessary to obtain the full capacity of sodium alanate. It is possible, although far from certain, that the size of the system contributes to this process, i. e. until all the modules in the tank reach the same status, a number of cycles is necessary. Since other authors do not report any activation cycles [10], this topic will need to be investigated further.

In the dehydrogenation process the dependency between hydrogen flow, pressure

and temperature is different from that of the hydrogenation. Whereas in the latter a constant pressure means that a limit is set to the temperature than can be used because of the equilibrium conditions having been reached [13], in the dehydrogenation the rate of desorption will be higher the higher the temperature is. The only limits for the temperature are those set by the vessel materials, the heat transfer system and the advisablility of not melting the sodium alanate ( $T_{\text{melting}} = 184$  °C). In the case of the equipment used in this investigation, the desorption temperature is limited by hardware to  $< 180$  °C, and we use  $160$  °C (see Fig. 5).

Fig. 5

In Fig. 5, the difference in permitted hydrogen flow is visible: in the case of the 16th desorption, the hydrogen output valve was opened more widely than for the others. Therefore, the total capacity curve in the 16th desorption is much steeper than for the other two desorptions after the initial stage, where the slope is determined by the maximum allowed flow of  $240 \text{ Ln min}^{-1}$ .

In order to directly observe the behaviour of the powder inside the tank under operating conditions, an imaging technique is desirable as a complement to the volumetric Sieverts' one just described. Due to the sensitivity of neutrons towards hydrogen, and their ability to penetrate the pressure hull of an hydrogen storage tank if made of aluminium, neutron radiography is the ideal technique for in situ imaging investigations. For these experiments a special  $165 \times 165$  mm large tank was used with a sample thickness of 6 mm, diameter of 105 mm and a 40 mm thick manganese-strengthened aluminium wall. The tank, equipped with heating cartridges and temperature sensors, is designed for operating conditions of 100 bars and  $180$  °C. Aluminium can easily be penetrated by neutrons while still offering enough mechanical strength. In order to avoid a possible activation of the chlorine atoms,  $\text{TiF}_3$  was selected as the dopant of choice in preference to the more known  $\text{TiCl}_3$  or  $\text{TiCl}_4$ . Although the fluoride has been shown to be less effective than the chlorides [13], this seems to be mainly dependent on the preparation route, and other authors have shown good behavior for alanate doped with the fluoride [14]. After conditioning of the tank at  $125$  °C, hydrogen was absorbed at the same temperature, using a pressure of 80 bar and at a slow hydrogen flow of first 25 and then  $50 \text{ mLn min}^{-1}$ , regulated by an automatic mass flow controller. For desorption a temperature of

160°C and a fast flow of several  $\text{L min}^{-1}$  were used. After the first absorption and desorption cycle, a second complete absorption was performed. Fig. 6 shows the results of the neutron radiography measurements on the  $\text{NaAlH}_4$  tank.

Fig. 6

The first graph, Fig. 6a, shows the material after filling (loose powder) and before any loading has taken place. Fig. 6b shows an intermediate stage of the loading, which was carried out at an initial pressure of 80 bar and 125 °C. A dendritic channel structure of free space has developed from the loading port in the lower left corner to the more distant powder particles. The darker color indicates that hydrogen, which interacts with neutrons rather powerfully, is already in the bulk. Fig. 6c is the final stage after charging with hydrogen, discharging and recharging once more. Although the alanate phase changes chemically during cycling the channel structure remained comparatively stable. However, the darker colour of the bulk material in Fig. 6b, and even more so in Fig. 6c shows that the hydrogen is homogeneously distributed. However, to optimize such a storage tank, the formation of channel structures has to be avoided, since it can prevent heat transfer from and to the inner part of the powder bed so that the sorption kinetics becomes slower. Neutron radiography shows that the channels are not necessary to charge the powder, so that capacity can be increased by compacting the powder instead of using it in a loose form.

### *Conclusions*

It can be concluded that the tank designed within the STORHY project fulfils the kinetics goals set, thereby validating the design and simulation work carried out previously. Moreover, the ease of use, speed of charging and result reproducibility of the 8 kg alanate tank have proven to be outstanding, paving the way to the application of hydrogen storage tanks based on complex hydrides wherever a source of waste heat compatible with the energy needs of the tank (especially regarding the temperature level) is available. This is the case especially in large scale and stationary applications. Neutron radiography has proven to be a reliable method to obtain images of the hitherto hidden inner regions of a hydrogen storage tank, and will be developed further. A use as a quality assurance testing tool may be possible.

## Acknowledgements

Financial support from the European Community under the Integrated Project “NESSHY – Novel Efficient Solid Storage for Hydrogen” (contract SES6 – CT – 2005 – 518271) is hereby thankfully acknowledged.

## References

- [1] Schlapbach L, Zuttel A. Hydrogen-storage materials for mobile applications. *Nature* 2001;414:353-358.
- [2] Zuttel A. Hydrogen storage methods. *Naturwissenschaften* 2004;91:157-172.
- [3] Strubel. Future Perspectives of Automotive Hydrogen Storage. vol. 2009. Paris, 2008. p.[http://www.storhy.net/finalevent/pdf/StorHy-Final-Event\\_PR.pdf](http://www.storhy.net/finalevent/pdf/StorHy-Final-Event_PR.pdf).
- [4] DOE. DOE Targets for Onboard Hydrogen Storage Systems for Light-Duty Vehicles. 2009.  
[https://www1.eere.energy.gov/hydrogenandfuelcells/storage/pdfs/targets\\_onboard\\_hydro\\_storage.pdf](https://www1.eere.energy.gov/hydrogenandfuelcells/storage/pdfs/targets_onboard_hydro_storage.pdf); [viewed 28.10.2010]
- [5] Commission E. Fuel Cells and Hydrogen Joint Technology Initiative. [http://ec.europa.eu/research/fch/index\\_en.cfm?pg=back](http://ec.europa.eu/research/fch/index_en.cfm?pg=back); [viewed 30.10.2010]
- [6] Na Ranong C, Höhne M, Franzen J, Hapke J, Fieg G, Dornheim M, Eigen N, Bellosta von Colbe J, Metz O. Concept, Design and Manufacture of a Prototype Hydrogen Storage Tank Based on Sodium Alanate. *Chemical Engineering & Technology* 2009;32:1154-1163.
- [7] Na Ranong C, Höhne M, Franzen J, Hapke J, Fieg G, Dornheim M. Modellgestützte verfahrenstechnische Berechnung eines Metallhydridspeichers auf Natriumalanatbasis im Technikumsmaßstab. *Chemie Ingenieur Technik* 2009;81:645-654.
- [8] Mosher DA, Arsenault S, Tang X, Anton DL. Design, fabrication and testing of NaAlH<sub>4</sub> based hydrogen storage systems. *Journal of Alloys and Compounds* 2007;446-447:707-712.
- [9] Eigen N, Keller C, Dornheim M, Klassen T, Bormann R. Industrial production of light metal hydrides for hydrogen storage. *Scripta Materialia* 2007;56:847-851.
- [10] Lozano GA, Eigen N, Keller C, Dornheim M, Bormann R. Effects of heat transfer on the sorption kinetics of complex hydride reacting systems. *International Journal of Hydrogen Energy* 2009;34:1896-1903.
- [11] Lozano GA, Ranong CN, Bellosta von Colbe JM, Bormann R, Fieg G, Hapke J, Dornheim M. Empirical kinetic model of sodium alanate reacting system (I). Hydrogen absorption. *International Journal of Hydrogen Energy* 2010;35:6763-6772.
- [12] Gross KJ, Majzoub EH, Spangler SW. The effects of titanium precursors on hydriding properties of alanates. *Journal of Alloys and Compounds* 2003;356:423-428.
- [13] Bellosta von Colbe JM, Bogdanovic B, Felderhoff M, Pommerin A, Schuth F. Recording of hydrogen evolution - a way for controlling the doping process of sodium alanate by ball milling. *Journal of Alloys and Compounds* 2004;370:104-109.
- [14] Andrei CM, Walmsley JC, Brinks HW, Holmestad R, Srinivasan SS, Jensen CM, Hauback BC. Electron-microscopy studies of NaAlH<sub>4</sub> with TiF<sub>3</sub> additive: hydrogen-cycling effects. *Applied Physics A: Materials Science & Processing* 2005;80:709-715.

Figure captions



Fig. 1 8 kg alanate hydrogen storage tank connected to the testing setup in the explosion-protected lab.

Fig. 2 Fast charging operation of the 8 kg alanate tank at 125 °C nominal temperature and pressure ranging from 3 to 100 bar. 12th cycle.

Fig. 3 Material and total capacity as well as H<sub>2</sub> flow and temperature vs. time for a typical absorption at 126 °C and pressure increasing from 1 to 109 bar with the H<sub>2</sub> flow capped at 240 Ln min<sup>-1</sup> nominal rate

Fig. 4 Comparison of three charging operations under the same conditions: 2 – 100 bar, 125 °C, 240 Ln min<sup>-1</sup> maximum hydrogen flow.

Fig. 5 Hydrogen desorption curves for cycles 16 to 18 at 160 °C and pressures going down to 0.2 barg. In cycle 16, the exhaust valve was opened by hand more widely than in cycles 17 and 18.

Fig. 6 Neutron radiography images of a sodium alanate hydrogen storage tank. a) initial state without hydrogen, b) filled with ca. 50 mLn H<sub>2</sub> during the first absorption, c) filled with ca. 20 Ln H<sub>2</sub> after dehydrogenation and renewed hydrogenation..

J.M. Bellosta von Colbe · Max Planck Str. 1 · 21502 Geesthacht

Prof. E. A. Veziroglu  
Editor in chief, International Journal of Hydrogen  
Energy  
1162 E. Sheffield Ave.  
Chandler, AZ 85225  
USA

Geesthacht, 19. November 2010

**Suggested reviewers for AIChE 2010 special edition**

Dear Prof. Veziroglu,

the suggested reviewers for this manuscript are:

1. Don Anton, Savannah River National Lab, USA
2. Terry A. Johnhson, Sandia National Labs, USA
3. Michael Felderhoff, Max Planck Institute for Coal Research, Germany,
4. Etsuo Akiba, AIST, Japan

With best regards,

José M. Bellosta von Colbe

Figure

[Click here to download high resolution image](#)



Figure  
[Click here to download high resolution image](#)

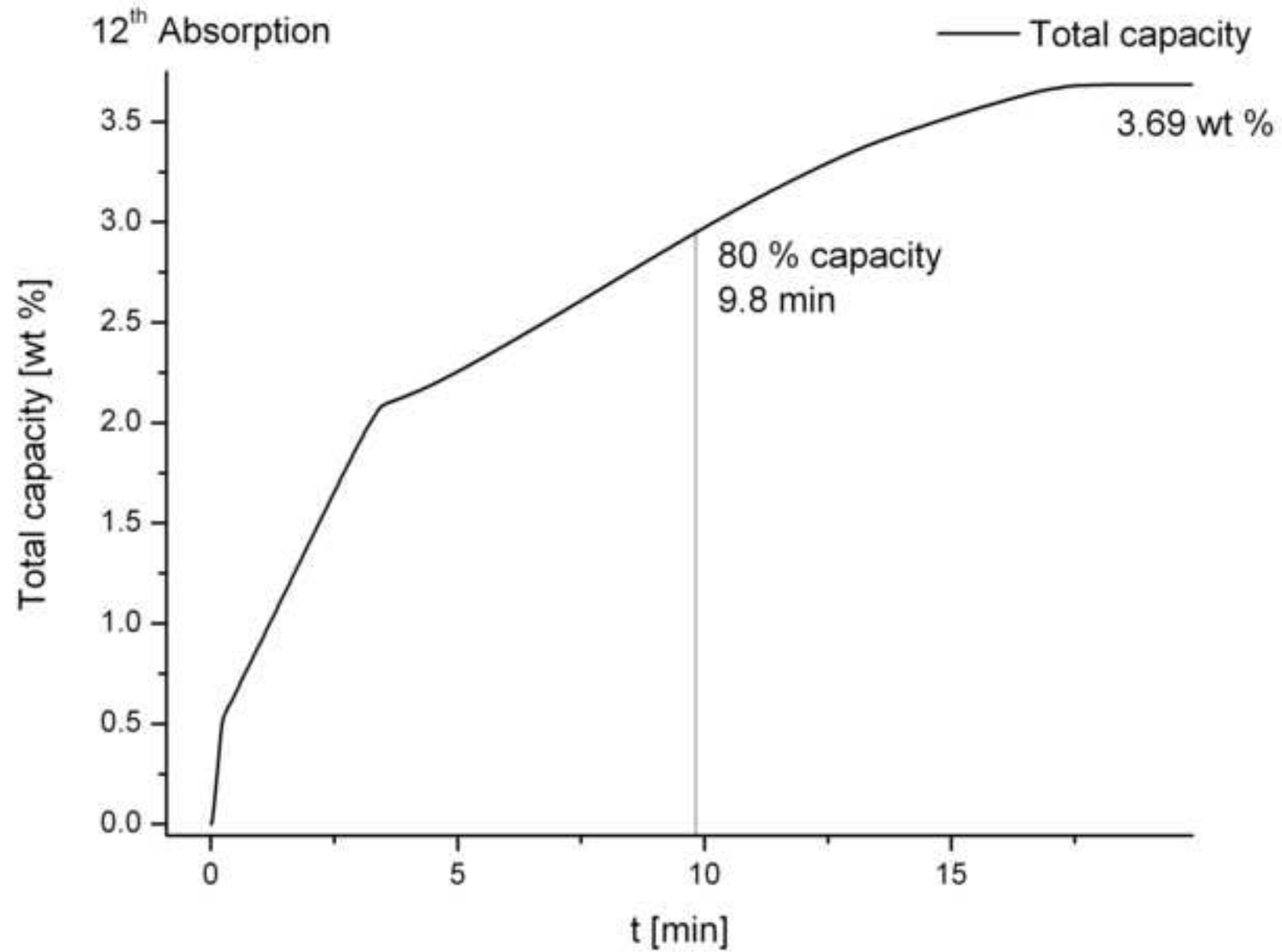


Figure  
[Click here to download high resolution image](#)

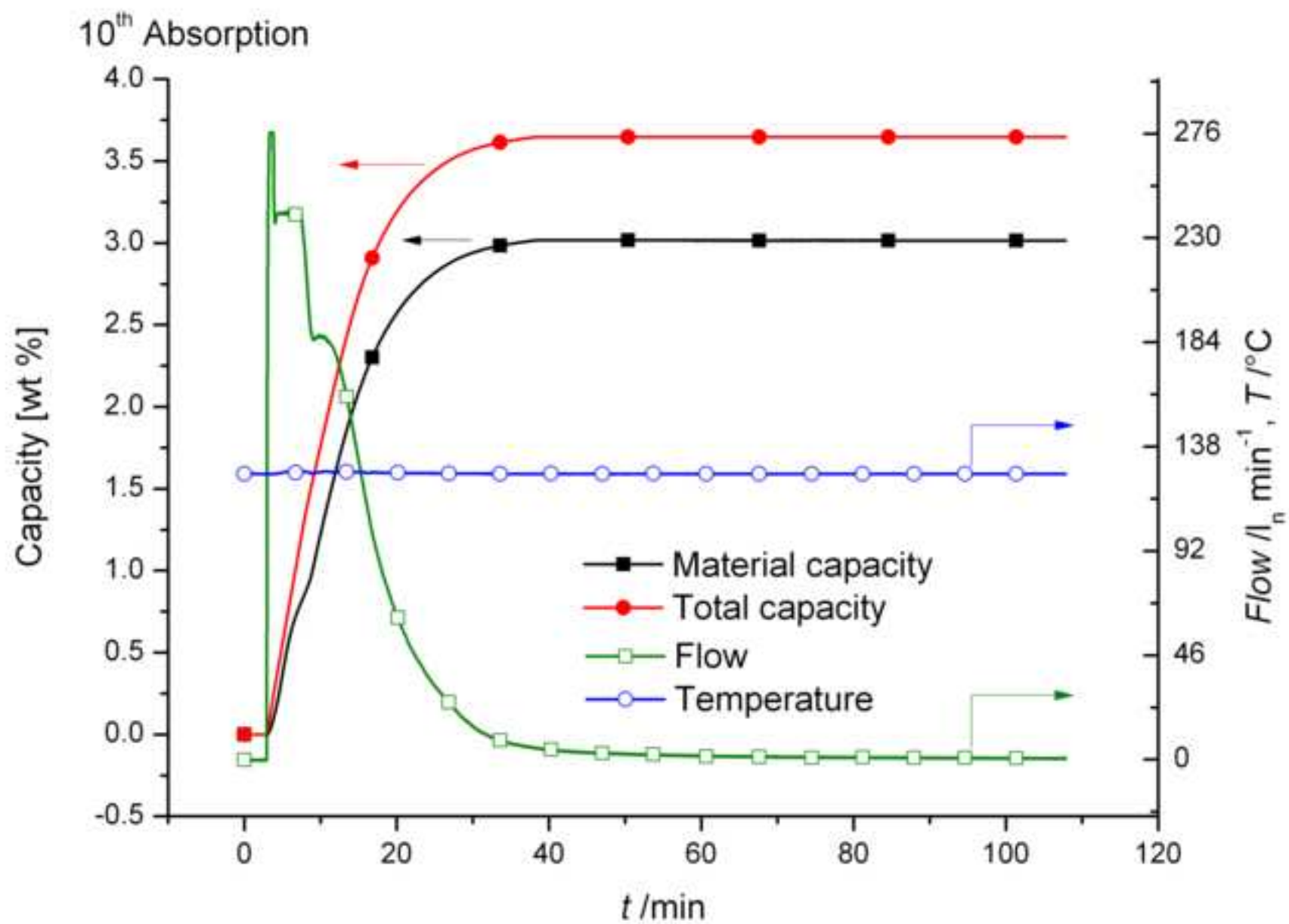


Figure  
[Click here to download high resolution image](#)

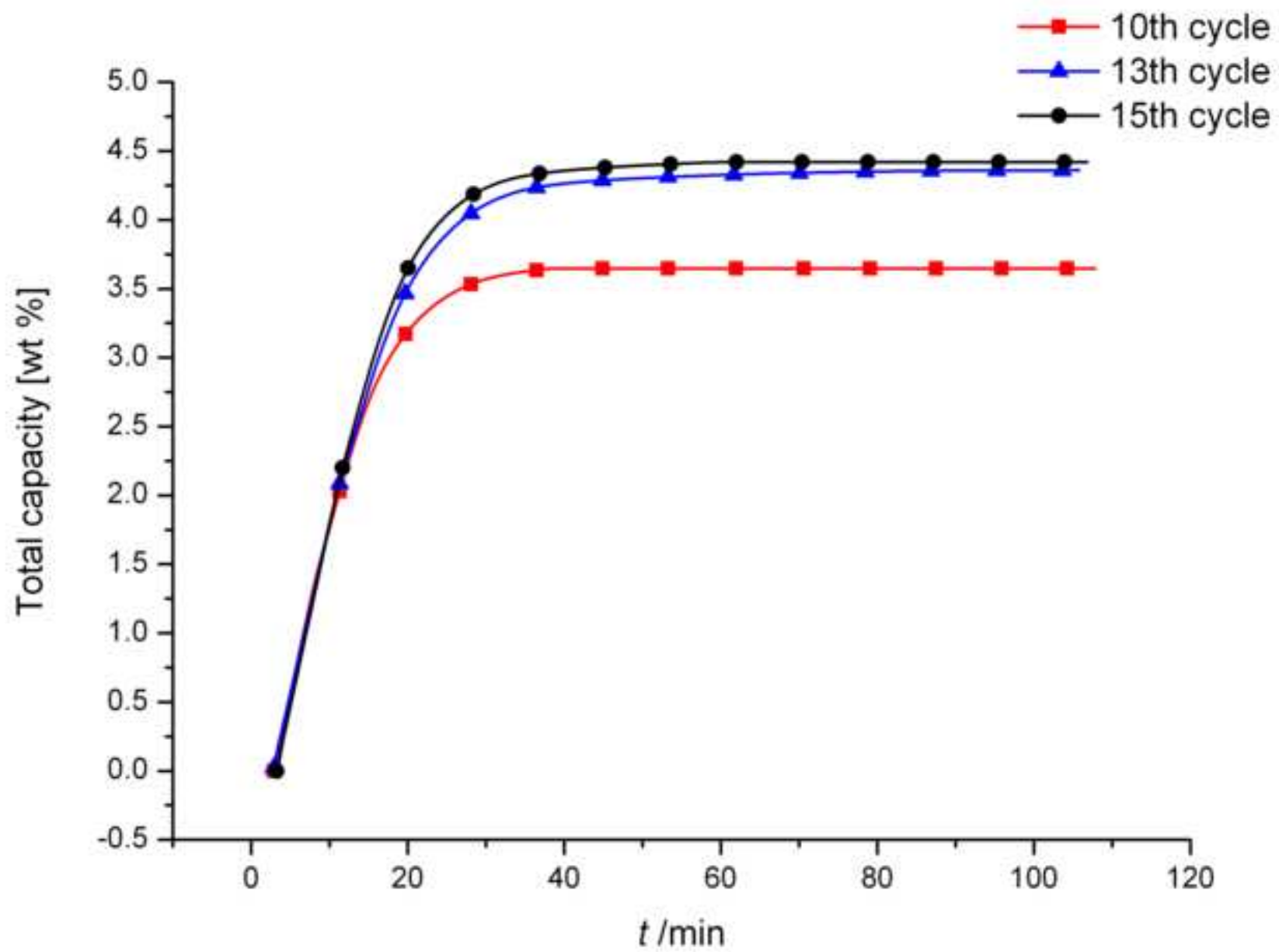
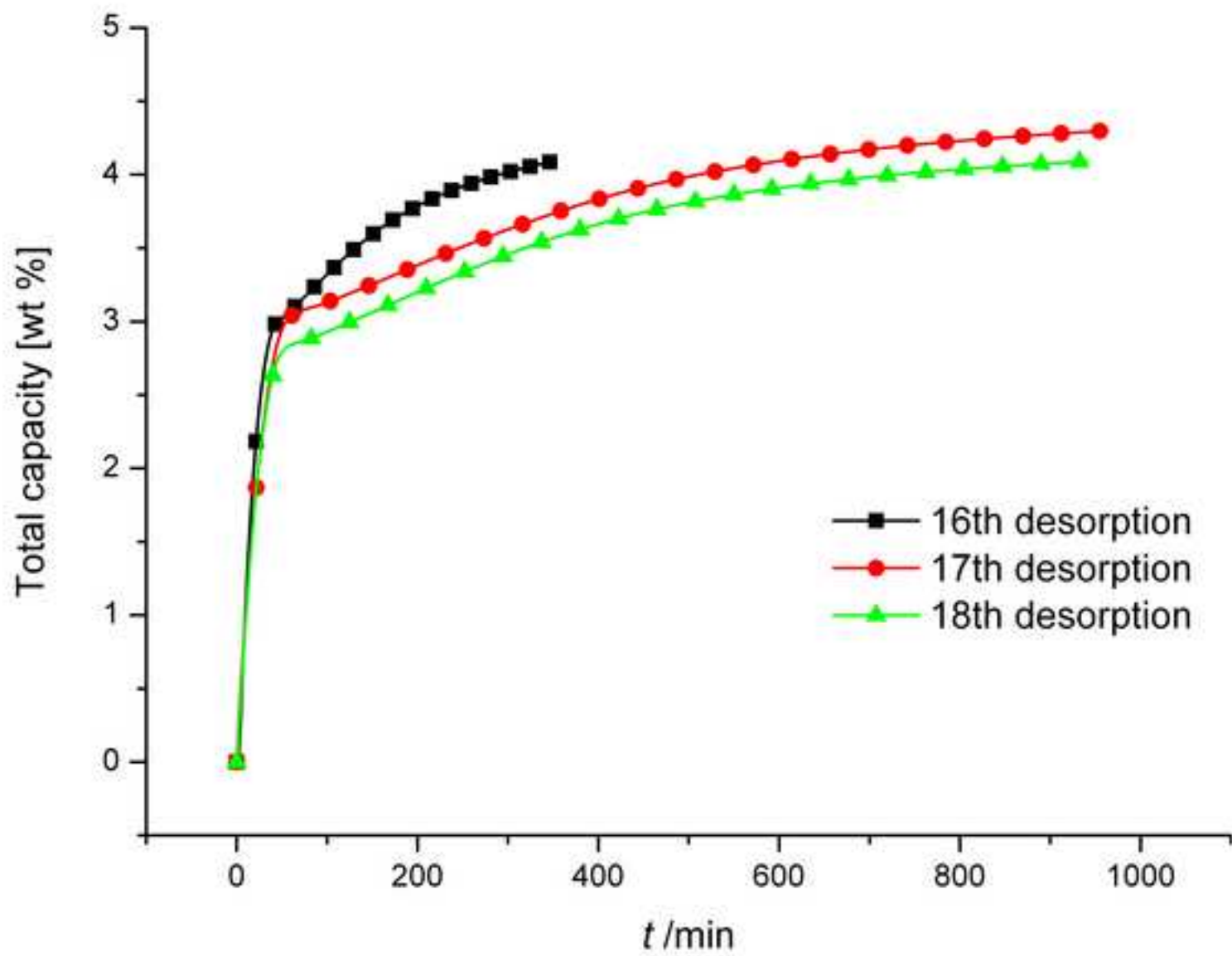


Figure  
[Click here to download high resolution image](#)



Figure

[Click here to download high resolution image](#)

